Research Article | Vol. 11, No. 1 / 1 January 2021 / Optical Materials Express 48
Optical Materials EXPRESS

Anionic fluorophore-assisted fabrication of gold microstructures inside a hydrogel by multi-photon photoreduction

MANAN MACHIDA,[1] WEILU SHEN,[2] HIROAKI ONOE,[1,3] YUKI HIRUTA,[1,4] ALEXANDER HEISTERKAMP,[1,5,6] ERIC MAZUR,[2,7] AND MITSUHIRO TERAKAWA[1,8,*]

[1]School of Integrated Design Engineering, Keio University, 3-14-1, Hiyoshi, Kohoku-ku, Yokohama 223-8522, Japan
[2]John A. Paulson School of Engineering and Applied Sciences, Harvard University, 9 Oxford Street, Cambridge, MA 02138, USA
[3]Department of Mechanical Engineering, Keio University, 3-14-1, Hiyoshi, Kohoku-ku, Yokohama 223-8522, Japan
[4]Department of Applied Chemistry, Keio University, 3-14-1, Hiyoshi, Kohoku-ku, Yokohama 223-8522, Japan
[5]Institut fuer Quantenoptik, Gottfried Wilhelm Leibniz University Hannover, Am Welfengarten 1, 30167 Hannover, Germany
[6]Industrial and Biomedical Optics Department, Laser Zentrum Hannover e.V., Hollerithallee 8, D-30419 Hannover, Germany
[7]Department of Physics, Harvard University, 9 Oxford Street, Cambridge, MA 02138, USA
[8]Department of Electronics and Electrical Engineering, Keio University, 3-14-1, Hiyoshi, Kohoku-ku, Yokohama 223-8522, Japan
*terakawa@elec.keio.ac.jp

Abstract: The fabrication of accentuated gold microstructures is demonstrated by multi-photon photoreduction inside an anionic fluorophore-containing hydrogel. We attempted to facilitate gold-ion photoreduction near the focal point of laser pulses, expecting the donation of electrons by the oxidation of fluorophores in the vicinity of gold ions. The presence of anionic FITC-dextran also inhibited the spontaneous reduction in untargeted zones, which is attributed to the coordination of gold ions and the anionic FITC-dextran. Simultaneous facilitation and inhibition are promising for the fabrication of dense metal microstructures in the targeted zone while maintaining the hydrogel's light permeability.

1. Introduction

Ultrafast laser processing enables three-dimensional (3D) micro- and nanofabrication by multi-photon absorption induced near the focal point of laser pulses. Various studies on the fabrication of 3D micro- and nanostructures have been reported, such as the formation of void structures inside a glass [1], refractive index modification [2], and photopolymerization of polymers [3,4]. Regarding high-precision processing based on multi-photon absorption, several studies have been reported, including the precise control of the laser beam shape [5]. Multi-photon polymerization of photosensitive polymers is a method used to fabricate 3D polymer structures obtained by the polymerization reaction of free radicals generated based on multi-photon absorption by photoinitiators. Studies on high spatial-resolution photopolymerization by stimulated emission depletion (STED)-aided multi-photon photopolymerization [6] or based on chemical approaches such as utilization of efficient photoinitiators [7,8] or crosslinkers [9] have been reported.

Multi-photon photoreduction is one of the methods used to fabricate 3D metal micro- and nanostructures [10–13]. There have been many studies to improve the spatial resolution of the

#412066 https://doi.org/10.1364/OME.412066
Journal © 2021 Received 8 Oct 2020; revised 24 Nov 2020; accepted 30 Nov 2020; published 7 Dec 2020

Optical Materials EXPRESS

fabrication. For example, one method features the functional groups in molecules around metal ions and in the surface of the photoreduced metals. Reduction of metal ions is facilitated by utilizing reductants, which are oxidizable materials, as electron donors. Ascorbic acid [14] or glycol aldehyde [15] can be used as a reductant in metal ion solutions to achieve photoreduction. Liu *et al.* demonstrated the fabrication of a freestanding silver double-helix array on glass coverslips using trisodium citrate as a reductant [16]. The line widths of the fabricated silver nanowires were decreased by adding n-decanoylsarcosine sodium (NDSS) as a metal growth inhibitor. Other studies on the fabrication of metal micro- and nanostructures with a surfactant [17] or an amino acid [18] as a metal growth inhibitor have also been reported. Multi-photon photoreduction with light-absorbing molecules has also been investigated because the optical absorbance of molecules around metal ions affects the metal-ion reduction [19–24]. Ishikawa *et al.* reported the fabrication of silver structures by focusing femtosecond laser pulses in a silver-ion and coumarin 440 ethanol solution, which resulted in a smaller diameter of the silver structures and required lower laser power to trigger the reduction of silver ions than those fabricated without coumarin 440 solutions [24].

Although the utilization of reductants or light-absorbing molecules facilitates the multi-photon photoreduction of metal ions, the zone where the photoreduction is facilitated is not limited to the focal point, which causes the undesired enhancement of metal nanoseed formation and crystal growth in the metals. In particular, the simultaneous induction of facilitation of metal-ion photoreduction near the focal point and inhibition of reduction in the untargeted zone is challenging when the supporting base materials are needed to hold the metal structures after fabrication.

Materials used as supporting base materials for the fabrication of metal micro- and nanostructures by multi-photon photoreduction enable wider applications of the fabricated metal structures. For example, soft materials having good flexibility and biocompatibility are promising supporting materials for functional metal microstructures with respect to the realization of novel flexible devices owing to their elasticity. Studies on the fabrication of metal structures by multi-photon photoreduction within gelatin [25], poly(ethylene glycol) diacrylate (PEGDA) [26–28], and a thermo-responsive poly-N-isopropylacylamide (PNIPAm) hydrogel [29] have been reported. These soft materials are promising for novel applications, including wearable or implantable devices as well as soft microrobots.

In this study, we demonstrate the fabrication of accentuated gold microstructures *via* multi-photon photoreduction inside a hydrogel containing anionic fluorophores. We attempt to induce the facilitation of metal-ion photoreduction near the focal point owing to the interaction between the fluorophores and high-intensity laser pulses. The inhibition of metal-ion reduction in zones outside of the focal point is also demonstrated by utilizing FITC-dextran, an anionic fluorophore. We discuss the effect of fluorophores' charge on the metal-ion reduction in a zone outside of the focal point by adding a FITC-dextran or a Rhodamine110, the latter of which is a cationic fluorophore.

2. Materials and methods

2.1. Material preparation

To fabricate the hydrogel, PEGDA (average molecular mass 4000, Polysciences, Inc., USA) and the photoinitiator Irgacure2959 (Sigma-Aldrich Co. LLC, USA) were used. PEGDA (0.1 g) was dissolved in 1 ml of pure water containing 1% photoinitiator and stirred for 10 min. The solution was placed in a mold and illuminated by a 365 nm wavelength UV lamp (6 W) for 20 min to induce photo-cross-linking. The cross-linked hydrogel, 5 mm in length, 3 mm in width, and 3 mm in thickness was stored in pure water overnight to remove any uncross-linked PEGDA and Irgacure2959 from the hydrogel.

Optical Materials EXPRESS

To fabricate gold gratings within a hydrogel containing pure water as a solvent, the cross-linked hydrogel was immersed in a gold (III) chloride (Sigma-Aldrich Co. LLC) aqueous solution (4 mg/ml) for 10 min to add gold ions; then, femtosecond laser pulses were focused on a spot within the hydrogel. To fabricate gold gratings within a hydrogel containing a fluorophore solution, the hydrogel was immersed in fluorescein isothiocyanate-dextran (FITC-dextran, average molecular mass 3000-5000, Sigma-Aldrich Co. LLC) solution or Rhodamine 110 chloride (Rhodamine110, average molecular mass 366.80, Sigma-Aldrich Co. LLC) solution for 1 h. Both fluorophore solutions were dissolved in pure water at varying concentrations of 10 μM, 100 μM, or 500 μM. The hydrogel containing each fluorophore solution was then immersed in a gold (III) chloride aqueous solution (4 mg/ml) for 10 min to add gold ions; subsequently, the femtosecond laser pulses were focused inside the hydrogel. To discuss the contributions of FITC and dextran in the experiment with respect to the fabrication of gold gratings, the hydrogel was immersed in dextran obtained from *Leuconostoc mesenteroides* (Dextran, average molecular mass 5000, Supelco, Inc., USA) solution for 1 h. Thereafter, the hydrogel was immersed in a gold (III) chloride aqueous solution (4 mg/ml) for 10 min to add gold ions. Femtosecond laser pulses were then focused inside the hydrogel. Dextran solutions were dissolved in pure water at concentrations of 10 μM, 100 μM, or 500 μM. Furthermore, to discuss the effect of the anionic charge on the experiment involving FITC-dextran, the hydrogel containing pure water as a solvent was immersed in various gold(III) chloride solutions with phosphate buffered saline (PBS, Sigma-Aldrich, Co. LLC) as a solvent (4 mg/ml) for 10 min, and femtosecond laser pulses were focused inside the hydrogel. The PBS solutions were prepared at concentrations of 1.51 mM, 15.1 mM, or 151 mM. For all experiments, the hydrogel was immersed in pure water overnight to remove residual gold ions, fluorophores, and dextran after femtosecond laser irradiation. Values of pH were measured with a pH meter (AS600, As One Corp., Japan).

2.2. Laser irradiation

Gold gratings were fabricated within a hydrogel by multi-photon photoreduction of gold ions using femtosecond laser pulses. Figure 1 presents a schematic illustration of the gold grating fabricated by multi-photon photoreduction. Laser pulses with a central wavelength of 522 nm, the second harmonic wave of a 1045-nm femtosecond laser oscillator (High Q-2-SHG, Spectra-Physics, Inc., USA) were used for the fabrication of gold gratings. The repetition rate and pulse duration of the output pulses were 63 MHz and 192 fs, respectively. A water immersion objective lens (numerical aperture (NA) 1.0, working distance 2.0 mm, Olympus, Japan) was used to focus the laser pulses at a 250 μm depth from the surface of the hydrogel. Gold gratings (700 μm × 700 μm) with 10 μm pitch between adjacent lines were fabricated using a computer-controlled three-axis encoded (XYZ) motorized stage with a scanning speed of 80 μm/s along the xy-plane.

2.3. Observations and optical property evaluation

The fabricated gold gratings inside the wet hydrogel were observed using an inverted transmission optical microscope (Eclipse Ti-E, Nikon, Japan). 10x (NA 0.45) magnification microscope objective was used for obtaining the microscope images of the fabricated gratings by a camera (DS-Ri1, Nikon) attached to the microscope. The obtained bright-field microscope images were converted to gray scale and were used to measure the image intensity profile along the lines perpendicular to the gold gratings in the y-axis direction.

The hydrogel was dried and thinned using a mortar and pestle, and then 100 nm-thick thin films were prepared by slicing the sample in an epoxy-molding compound. The slices were then observed by transmission electron microscopy (TEM, Tecnai G2, FEI, USA). Elemental analysis of the fabricated structures formed from gold was performed by energy dispersive X-ray (EDX) spectroscopy during the scanning TEM. For the optical property evaluation of

Optical Materials EXPRESS

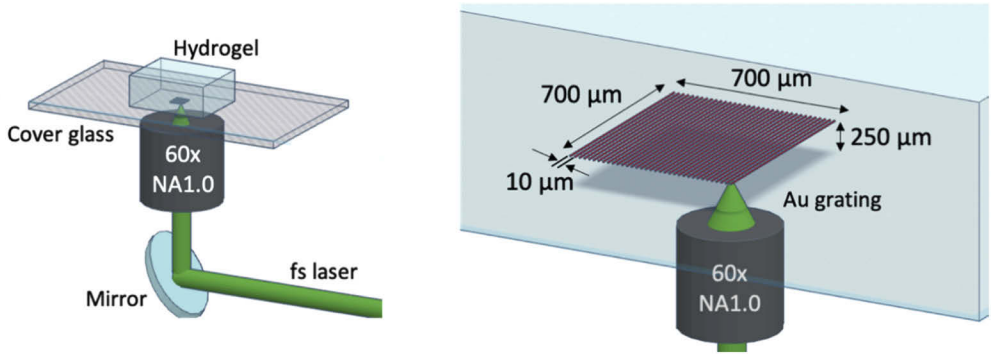

Fig. 1. Schematic illustration of a gold grating fabricated within a hydrogel by multi-photon photoreduction.

the fabricated gratings and the hydrogel, optical absorbance spectra were measured using a spectrometer (USB4000, Ocean Optics, Inc., USA).

3. Results and discussion

We attempted to fabricate gold microstructures *via* multi-photon photoreduction inside a hydrogel with ionic-charged fluorophores to induce the facilitation of metal-ion photoreduction near the focal point and inhibit reduction in zones outside of the focal point simultaneously.

Figure 2(a) shows the gold grating fabricated inside a fluorophore-free hydrogel by multi-photon photoreduction. The fabricated gold grating, with 10 µm pitch between adjacent lines, shows non-uniform line widths. A reddish color was observed in the fabricated gold grating and the hydrogel around the grating, which is attributable to the surface plasmon resonance of the gold nanoparticles. Because the entire hydrogel exhibits a reddish color, as shown in the optical image (inset of Fig. 2(a)), it was confirmed that gold ions were also reduced in the zones outside of the focal point of the laser pulses. Figures 2(b)–2(d) show the hydrogels containing the gold gratings that were fabricated by focusing femtosecond laser pulses after the hydrogels were immersed in FITC-dextran solutions with varying concentrations. We confirmed that the higher concentration of FITC-dextran solution, the larger the line width of the gold grating formed within a hydrogel. This result suggests that the gold-ion reduction was facilitated near the focal points of the laser pulses. In contrast, the inset optical images indicate that the reddish color throughout the entire hydrogel was lighter in the case of the lower concentrations of FITC-dextran solutions, which suggests that the FITC-dextran inhibits the gold-ion reduction in zones outside of the focal point. Figures 2(e)–2(g) show the hydrogels containing the gold gratings fabricated by focusing femtosecond laser pulses after immersion of hydrogels in Rhodamine110 solutions with different concentrations. We confirmed that the higher the concentration of Rhodamine110 solution, the larger the line width of the gold grating formed within a hydrogel, which indicates that gold-ion photoreduction was facilitated near the focal point by utilizing Rhodamine110, similar to the case when using FITC-dextran. In contrast to the case of FITC-dextran, the inset optical images indicate that the reddish color throughout the entire hydrogel was darker for higher concentrations of Rhodamine110 solution compared to hydrogels with lower concentrations of Rhodamine110. The results indicate that the zone where the gold-ion reduction was facilitated was not limited to the focal point in the case of Rhodanine110, as opposed to FITC-dextran. Figure 2(h) shows the intensity profiles of bright-field microscope images along the lines perpendicular to the gold gratings fabricated in hydrogels with FITC-dextran or Rhodamine110 solutions at a concentration of 500 µM. The intensity data obtained from the fluorophore-free hydrogel are

Optical Materials EXPRESS

also shown in Fig. 2(h). A significant difference in the intensity was observed between a gold line and the zone between gold lines in the FITC-dextran-containing hydrogel (hereinafter called "FITC-dextran hydrogel"), which is attributable to the facilitation of gold-ion photoreduction near the focal point and the inhibition of reduction in zones outside of the fabricated gold gratings. Although a difference in the intensity was also observed for the Rhodamine110-containing hydrogel (hereinafter called "Rhodamine110 hydrogel"), the intensity was comparably higher at all positions, which is explainable by the facilitation of gold-ion photoreduction within the entire hydrogel, as shown in the inset of Figs. 2(e)–2(g). In the case of the fluorophore-free hydrogel, a comparably lower difference in the amplitude of the intensity was observed from the zones outside of the gold microstructures. The line widths, which were derived from the full width at half maximum (FWHM) of the intensity peaks, were ~3.2 μm, ~2.6 μm, and ~1.3 μm for the FITC-dextran hydrogel, the Rhodamine110 hydrogel, and the fluorophore-free hydrogel, respectively.

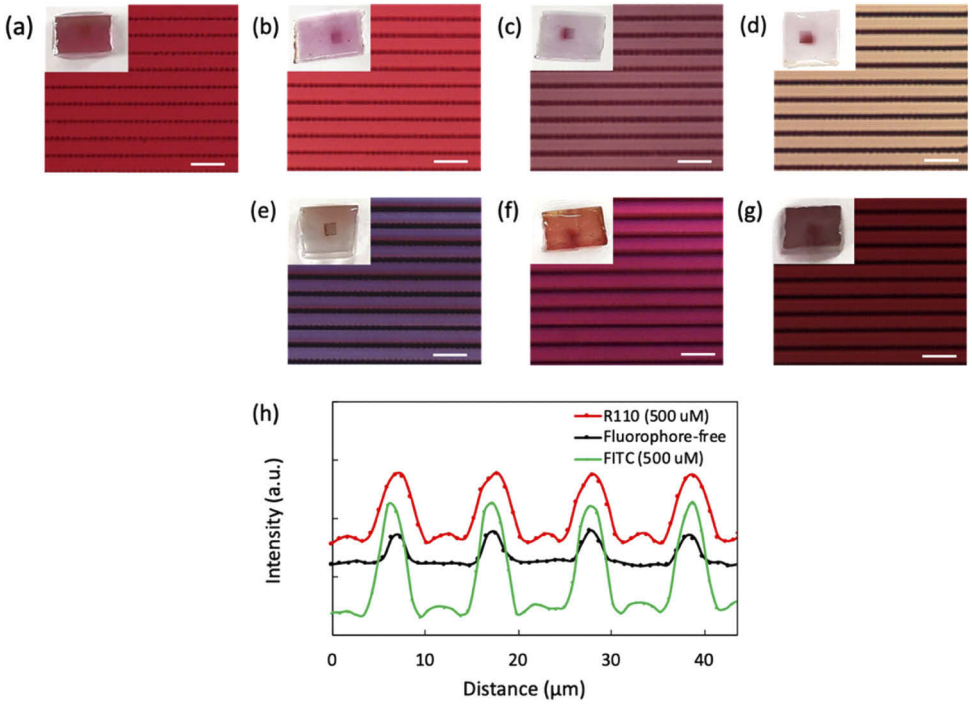

Fig. 2. Bright-field microscope images of fabricated gold gratings inside hydrogel containing fluorophores. The insets represent optical images of the hydrogels (5 mm × 3 mm × 3 mm). (a) Fluorophore-free hydrogel, (b)–(d) FITC-dextran hydrogels, (e)–(g) Rhodamine110 hydrogels. The concentrations of the fluorophores were (b) and (e): 10 μM, (c) and (f): 100 μM, (d) and (g): 500 μM, respectively. The scale bars represent 20 μm. (h) Intensity profiles of grayscale images converted from the microscope images shown in (a), (d), and (g) along the lines perpendicular to the gold gratings.

Because FITC-dextran is a molecular structure in which FITC is conjugated to dextran, we investigated the fabrication of gold gratings within a hydrogel immersed in dextran solutions to discuss the effect of FITC, which is a fluorescent molecule (Fig. 3). Neither a significant increase in the line widths nor an improvement in the line width uniformity was observed for any concentration of dextran solution in comparison with the case of the fluorophore-free hydrogel. Furthermore, the inset optical images exhibit a comparable reddish color, which is independent

Optical Materials EXPRESS

of the concentrations of the dextran solution used. Inhibition of gold-ion reduction was not observed, as opposed to the FITC-dextran hydrogel. These results indicate that the simultaneous induction of the facilitation of gold-ion photoreduction near the focal point and the inhibition of the reduction outside of the focal point is attributable to the presence of FITC.

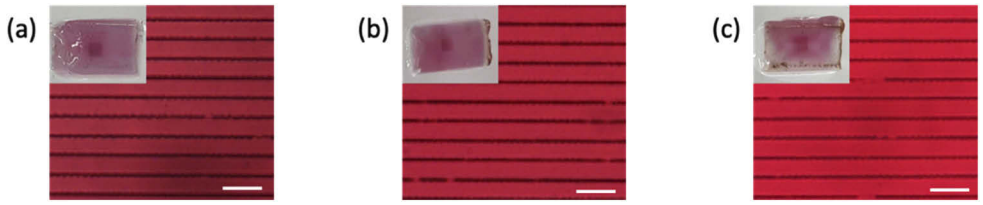

Fig. 3. Bright-field microscope images of fabricated gold gratings inside hydrogel containing a dextran solution. The insets represent the optical images of the hydrogels. The concentration of dextran solution is (a) 10 μM, (b) 100 μM, and (c) 500 μM, respectively. The scale bars represent 20 μm.

Figure 4 shows the optical absorbance spectra of the fabricated gold gratings within hydrogels immersed in FITC-dextran solutions or Rhodamine110 solutions. The absorbance peak of the gold grating fabricated within a fluorophore-free hydrogel was observed at approximately 560 nm, which is consistent with the typical resonant wavelengths of gold nanoparticles with a diameter from 80 to 90 nm [30]. In the case of a fluorophore-free hydrogel reported in our previous paper [28], we confirmed that gold nanoparticles with a diameter smaller than 10 nm and gold nanoparticle clusters with a diameter larger than 100 nm were formed. The absorbance peak observed is probably due to the overlapped spectra of the small nanoparticles and the nanoparticle clusters within a fluorophore-free hydrogel. The absorbance peak intensity of the gold grating fabricated within a FITC-dextran hydrogel increased as the concentration of the FITC-dextran solution increased (Fig. 4(a)). The absorbance peak intensity of the gold grating fabricated at an FITC-dextran solution concentration of 500 μM was 3.3 times as high as that fabricated within a fluorophore-free hydrogel. The spectra of the gold gratings fabricated with FITC-dextran shifted to shorter wavelengths. The absorbance peak of the gold grating fabricated at an FITC-dextran concentration of 500 μM exhibited a blue shift of approximately 10 nm compared to the peak of the grating within a fluorophore-free hydrogel, which was approximately 550 nm. This result suggests that the average diameter of the gold nanoparticles decreased, and the number of nanoparticles increased because of the presence of FITC-dextran in comparison with a fluorophore-free hydrogel.

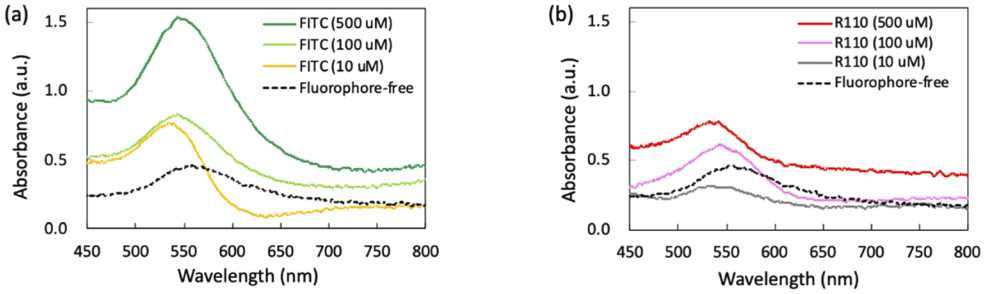

Fig. 4. Absorbance spectra of gold gratings fabricated in (a) FITC-dextran hydrogel and (b) Rhodamine110 hydrogel.

The absorbance peak intensity of the gold grating fabricated within a Rhodamine110 hydrogel also increased as the concentration of the Rhodamine110 solution increased (Fig. 4(b)). The result

Optical Materials EXPRESS

indicates that the number of gold nanoparticles formed near the focal point increased because of the presence of Rhodamine110 molecules as was the case for FITC-dextran. Although the degree of the increase in the absorbance peak intensity was lower than that of FITC-dextran, the absorbance peak intensity of the gold grating fabricated using a Rhodamine110 solution concentration of 500 μM was 1.7 times higher than that of a fluorophore-free hydrogel. As with the FITC-dextran, the absorbance spectra of the gold gratings fabricated with Rhodamine110 solutions shifted to shorter wavelengths compared to the fluorophore-free hydrogel, which suggests that the average diameter of the gold nanoparticles formed by multi-photon photoreduction decreased because of the presence of Rhodamine110. We confirmed that the fabricated gold gratings in hydrogels retained their shapes and optical properties over a week after the fabrication.

Figure 5 shows a TEM image and elemental analysis of the nanoparticles fabricated by multi-photon photoreduction in the presence of FITC-dextran. The aggregation of nanoparticles with diameters ranging from 5 to 30 nm was observed. The nanoparticles were formed densely in comparison with the case of the fluorophore-free hydrogel reported in our previous paper [28]. Nanoparticle clusters with diameters larger than 100 nm were not observed as in the previous case for fluorophore-free hydrogel. Photobleaching reactions of fluorophores are known to be induced by high-intensity light irradiation [31]. The photobleaching reaction accompanies the oxidation of the fluorophores, that is, free electrons are donated to molecules in the vicinity. It is suggested that the facilitation of gold-ion photoreduction occurs when the free electrons are donated to gold ions that exist around the fluorophores. A large number of gold nanoparticles with a diameter of 5 nm were formed around the gold gratings, while gold nanoparticle clusters larger than 100 nm were not observed. The TEM image indicates that the nuclei of metal atoms were notably generated, whereas the growth of metal nanoparticles was inhibited, which is consistent with the results shown in Fig. 4. The generation of metal nuclei is considered to be facilitated primarily through the donation of free electrons from the photobleached fluorophores to gold ions, resulting in the formation of dense seed gold nanoparticles. The local heating of gold nanoparticles due to surface plasmon absorption facilitates the growth of metal nanoparticles and clusters by the thermal reduction of metal ions; however, the laser energy is distributed among the fluorophore molecules in the case of the fluorophore-containing hydrogel, which may decrease the energy provided for the growth of nanoparticles.

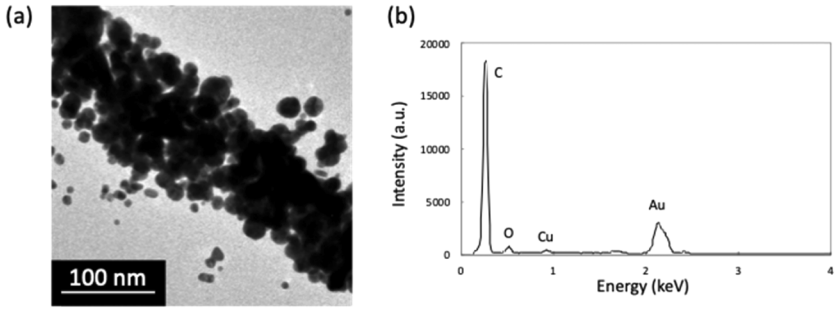

Fig. 5. (a) TEM image of metal nanoparticles formed in the gold grating within a FITC-dextran hydrogel. The laser power and scanning speed for multi-photon photoreduction were 4 mW and 80 μm/s, respectively. (b) EDX analysis of a point on a nanoparticle.

Figure 6 shows the optical absorbance spectra at a position sufficiently distant from the gold grating (~1 mm from the gold grating) in the hydrogels containing the gold gratings fabricated by focusing femtosecond laser pulses after immersion of hydrogels in FITC-dextran or Rhodamine110 solutions. The absorbance peak of the fluorophore-free hydrogel containing fabricated gold gratings was observed at approximately 547 nm, which indicates that the gold

Optical Materials EXPRESS

nanoparticles were also generated in zones outside of the focal point of the laser pulses. In addition to the spontaneous reduction of metal ions, light scattering may also induce a reduction in zones outside of the focal point of the laser pulses. The absorbance peak intensity of the FITC-dextran hydrogel decreased as the concentration of FITC-dextran solution increased (Fig. 6(a)). A broad range of absorbance and comparably lower absorbance was obtained at the measured wavelengths of the FITC-dextran hydrogel with a concentration of 500 μM. In contrast, the absorbance peak intensity of the Rhodamine110 hydrogel increased as the concentration of Rhodamine110 solution increased (Fig. 6(b)).

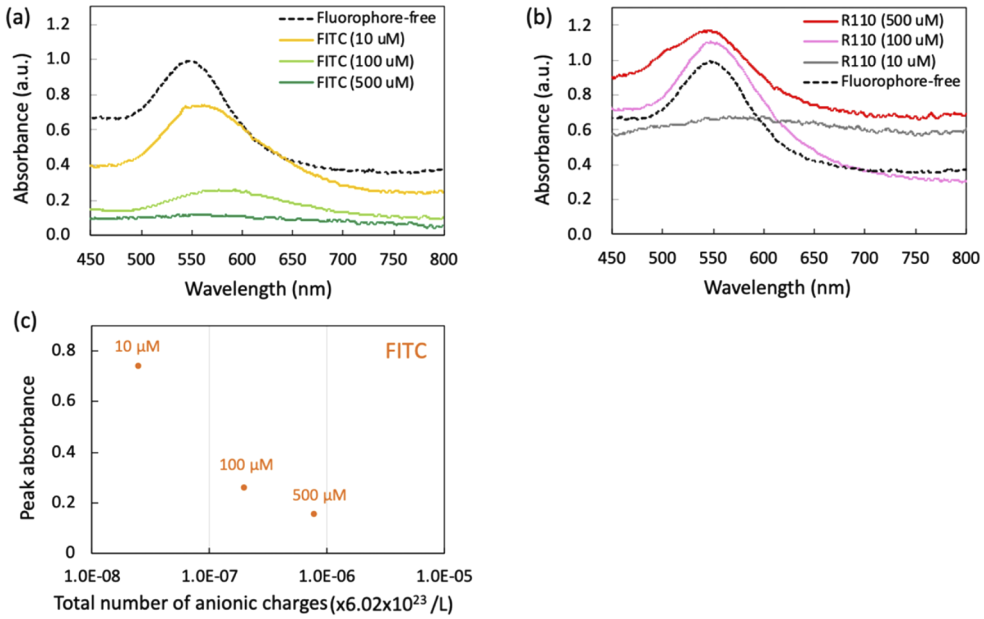

Fig. 6. Absorbance spectra of (a) FITC-dextran hydrogels and (b) Rhodamine110 hydrogels after laser irradiation in the fabrication of gold gratings. (c) The dependence of the absorbance peak intensity of the hydrogels on the estimated possible maximum total number of anionic charges of solutions.

The reduction of gold ions is significantly related to the charge of the molecules around the gold ions. Fluorescent FITC-dextran behaves as an anionic or deprotonated fluorophore, whereas fluorescent Rhodamine110 behaves as a cationic fluorophore within hydrogels. We investigated the dependence of the absorbance peak intensity of hydrogels on the possible maximum total number of anionic charges of the FITC-dextran solution, as shown in Fig. 6(c), to discuss the effect of the charge on the inhibition of gold-ion reduction within a hydrogel. The degree of ionization of FITC-dextran solutions of each concentration was estimated using the Henderson-Hasselbalch equation [32]:

$$pH = pK_a + \log[A^-]/[HA] \tag{1}$$

where pH is a value that was measured from FITC-dextran solutions with varying concentration, and pK_a is 6.4, and is a constant value for FITC-dextran. The possible maximum total numbers of anionic charges for each concentration of FITC-dextran were calculated by taking into account that the FITC part can be considered as dianionic when the degree of ionization of FITC-dextran is 1. Figure 6(c) shows that the absorbance peak intensity of the hydrogel decreased as the possible maximum total number of anionic charges in the FITC-dextran solutions increased. This result suggests that the rate of gold-ion reduction decreased because of the coordination of

Optical Materials EXPRESS

residual gold ions and the dianionic FITC-dextran. Gold ion-coordinated FITC-dextran can be removed by water immersion of the hydrogel after the fabrication of gold gratings overnight.

To discuss and support the hypothesis that anionic charges inhibit gold-ion reduction, we investigated the fabrication of gold gratings within a hydrogel by using $AuCl_3$ solutions prepared with PBS solution as a solvent (Figs. 7(a)–7(c)). The reddish color of the entire hydrogel was lighter as the concentration of the PBS solution increased. The absorbance peak intensity of a position sufficiently distant from the gold grating (~1 mm from the gold grating) in the hydrogel decreased as the concentration of PBS solution increased (Fig. 7(d)), which is consistent with the FITC-dextran results. The dependence of the absorbance peak intensity of the hydrogels on the possible maximum total number of anionic charges of $AuCl_3$ solutions was derived, as shown in Fig. 7(e). The pH values of the $AuCl_3$ solutions for each concentration were measured. It was confirmed that the absorbance peak intensity of the hydrogels decreased as the possible maximum total number of anionic charges in the PBS solution increased, which indicated that the inhibition of gold-ion reduction in a zone outside of the focal point is attributable to the number of anionic charges. In contrast, neither a significant increase in line width nor an improvement in the line width uniformity was observed in the case of the PBS solutions, which differed from the FITC-dextran results.

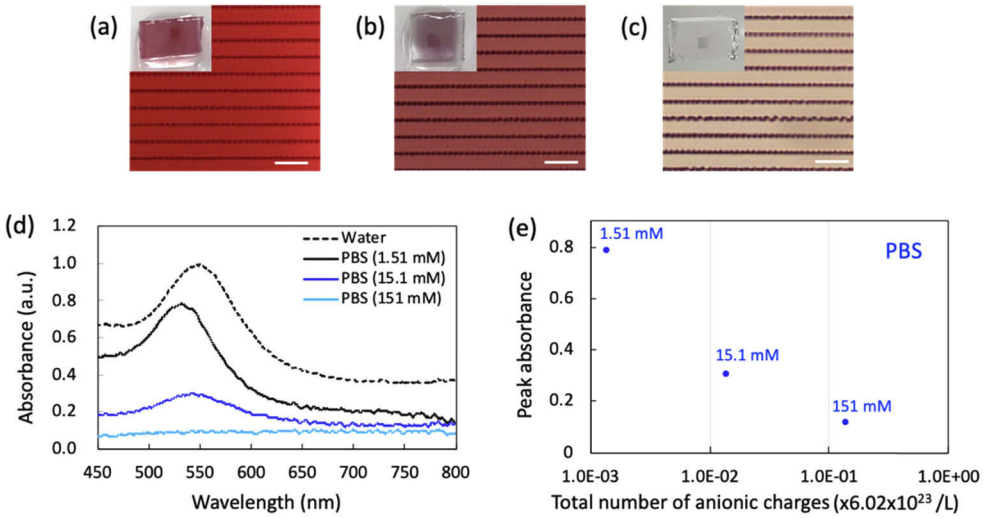

Fig. 7. Fabricated gold gratings inside a hydrogel using PBS as the solvent for $AuCl_3$ solutions. (a)–(c) Bright-field microscope images of fabricated gold gratings. The insets represent the optical images of the hydrogels. The concentrations of PBS are (a) 1.51 mM, (b) 15.1 mM, and (c) 151 mM, respectively. The scale bars represent 20 μm. (d) Absorbance spectra of the hydrogels after laser irradiation in the fabrication of gold gratings with PBS. (e) The dependence of the peak absorbance of the hydrogels on the estimated possible maximum total number of anionic charges in the solutions.

By utilizing FITC-dextran, the oxidation of the fluorophores that accompanies photobleaching facilitates the photoreduction of gold ions, which is explainable based on the donation of free electrons from fluorophores to gold ions. The inhibition of gold-ion reduction was induced because of anionic charges on the gold ions, which is attributable to the coordination of residual gold ions and the dianionic FITC-dextran. Although the inhibition of gold-ion reduction occurs simultaneously owing to the coordination of gold ions and the anionic charged molecules, the facilitation of gold-ion photoreduction appears to be significantly dominant.

Optical Materials EXPRESS

4. Conclusion

We have demonstrated the fabrication of accentuated gold gratings *via* multi-photon photoreduction within a hydrogel with anionic FITC-dextran. The gold-ion photoreduction was facilitated near the focal point within the fluorophore-containing hydrogels. Because the photobleaching reaction of fluorophores that accompanies the oxidation of fluorophores is known to be induced by high-intensity light irradiation, the facilitation of gold-ion photoreduction can occur by the donation of the free electrons from photobleached fluorophores to gold ions near the focal point. Furthermore, the gold-ion reduction in zones outside of the focal point was inhibited by utilizing anionic FITC-dextran, which is contrary to the case when using cationic Rhodamine110. The results suggest that the rate of gold-ion reduction decreased because of the coordination of gold ions and the dianionic charges in FITC-dextran. The fabrication of metal microstructures within a hydrogel containing an anionic fluorophore is a promising technique for the dense generation of metal nanoparticles while inhibiting the reduction of gold ions in untargeted zones within a hydrogel, which will contribute to the fabrication of soft flexible devices.

Funding

Ministry of Education, Culture, Sports, Science and Technology (MEXT) KAKENHI (JP18H03551); Japan Society for the Promotion of Science Grant-in-Aid for JSPS Fellows (JP20J13150).

Disclosures

The authors declare no conflicts of interest.

References

1. K. Sugioka and Y. Cheng, "Fabrication of 3D microfluidic structures inside glass by femtosecond laser micromachining," Appl. Phys. A **114**(1), 215–221 (2014).
2. K. M. Davis, K. Miura, N. Sugimoto, and K. Hirao, "Writing waveguides in glass with a femtosecond laser," Opt. Lett. **21**(21), 1729–1731 (1996).
3. S. Maruo, O. Nakamura, and S. Kawata, "Three-dimensional microfabrication with two-photon-absorbed photopolymerization," Opt. Lett. **22**(2), 132–134 (1997).
4. L. Li and J. T. Fourkas, "Multiphoton polymerization," Mater. Today **10**(6), 30–37 (2007).
5. F. He, H. Xu, Y. Cheng, J. Ni, H. Xiong, Z. Xu, K. Sugioka, and K. Midorikawa, "Fabrication of microfluidic channels with a circular cross section using spatiotemporally focused femtosecond laser pulses," Opt. Lett. **35**(7), 1106–1108 (2010).
6. M. T. Raimondi, S. M. Eaton, M. M. Nava, M. Laganà, G. Cerullo, and R. Osellame, "Two-photon laser polymerization: from fundamentals to biomedical application in tissue engineering and regenerative medicine," J. Appl. Biomater. Funct. Mater. **10**(1), 55–66 (2012).
7. M. Malinauskas, A. Žukauskas, G. Bičkauskaitė, R. Gadonas, and S. Juodkazis, "Mechanisms of three-dimensional structuring of photo-polymers by tightly focussed femtosecond laser pulses," Opt. Express **18**(10), 10209–10221 (2010).
8. J.-F. Xing, X.-Z. Dong, W.-Q. Chen, X.-M. Duan, N. Takeyasu, T. Tanaka, and S. Kawata, "Improving spatial resolution of two-photon microfabrication by using photoinitiator with high initiating efficiency," Appl. Phys. Lett. **90**(13), 131106 (2007).
9. V. F. Paz, M. Emons, K. Obata, A. Ovsianikov, S. Peterhänsel, K. Freneer, C. Reinhardt, B. Chichkov, U. Morgner, and W. Osten, "Development of functional sub-100 nm structures with 3D two-photon polymerization technique and optical methods for characterization," J. Laser Appl. **24**(4), 042004 (2012).
10. T. Tanaka, A. Ishikawa, and S. Kawata, "Two-photon-induced reduction of metal ions for fabricating three-dimensional electrically conductive metallic microstructure," Appl. Phys. Lett. **88**(8), 081107 (2006).
11. S. Maruo and T. Saeki, "Femtosecond laser direct writing of metallic microstructures by photoreduction of silver nitrate in a polymer matrix," Opt. Express **16**(2), 1174–1179 (2008).
12. N. Tsutsumi, K. Nagata, and W. Sakai, "Two-photon laser fabrication of three-dimensional silver microstructures with submicron scale linewidth," Appl. Phys. A **103**(2), 421–426 (2011).
13. K. Vora, S. Y. Kang, S. Shukla, and E. Mazur, "Fabrication of disconnected three-dimensional silver nanostructures in a polymer matrix," Appl. Phys. Lett. **100**(6), 063120 (2012).
14. T. S. Rodrigues, M. Zhao, T.-H. Yang, K. D. Gilroy, A. G. M. da Siva, P. H. C. Camargo, and Y. Xia, "Synthesis of colloidal metal nanocrystals: a comprehensive review on the reductants," Chem. - Eur. J. **24**(64), 16944–16963 (2018).

Optical Materials EXPRESS

15. S. E. Skrabalak, B. J. Wiley, M. Kim, E. V. Formo, and Y. Xia, "On the polyol synthesis of silver nanostructures: glycolaldehyde as a reducing agent," Nano Lett. **8**(7), 2077–2081 (2008).
16. L. Liu, D. Yang, W. Wan, H. Yang, Q. Gong, and Y. Li, "Fast fabrication of silver helical metamaterial with single-exposure femtosecond laser photoreduction," Nanophotonics **8**(6), 1087–1093 (2019).
17. Y.-Y. Cao, N. Takeyasu, T. Tanaka, X.-M. Duan, and S. Kawata, "3D metallic nanostructure fabrication by surfactant-assisted multiphoton-induced reduction," Small **5**(10), 1144–1148 (2009).
18. X.-L. Ren, M.-L. Zheng, F. Jin, Y.-Y. Zhao, X.-Z. Dong, J. Liu, H. Yu, X.-M. Duan, and Z.-S. Zhao, "Laser direct writing of silver nanowire with amino acids-assisted multiphoton photoreduction," J. Phys. Chem. C **120**(46), 26532–26538 (2016).
19. M. H. Hong, B. Luk'yanchuk, S. M. Huang, T. S. Ong, L. H. Van, and T. C. Chong, "Femtosecond laser application for high capacity optical data storage," Appl. Phys. A **79**(4-6), 791–794 (2004).
20. N. Tosa, J. Bosson, G. Vitrant, P. Baldeck, and O. Stephan, "Fabrication of metallic nanowires by two-photon absorption," Sci. St. Research VII **4**, 899–904 (2006).
21. N. Tosa, J. Bosson, M. Pierre, C. Rambaud, M. Bouriau, G. Vitrant, O. Stéphan, S. Astilean, and P. L. Baldeck, "Optical properties of metallic nanostructures fabricated by two- photon induced photoreduction," Proc. SPIE **6195**, 619501 (2006).
22. K. Terzaki, N. Vasilantonakis, A. Gaidukeviciute, C. Reinhardt, C. Fotakis, M. Vamvakaki, and M. Farsari, "3D conducting nanostructures fabricated using direct laser writing," Opt. Mater. Express **1**(4), 586–597 (2011).
23. S. Shukla, X. Vidal, E. P. Furlani, M. T. Swihart, K.-T. Kim, Y.-K. Yoon, A. Urbas, and P. N. Prasad, "Subwavelength direct laser patterning of conductive gold nanostructures by simultaneous photopolymerization and photoreduction," ACS Nano **5**(3), 1947–1957 (2011).
24. A. Ishikawa, T. Tanaka, and S. Kawata, "Improvement in the reduction of silver ions in aqueous solution using two-photon sensitive dye," Appl. Phys. Lett. **89**(11), 113102 (2006).
25. S. Y. Kang, K. Vora, and E. Mazur, "One-step direct-laser metal writing of sub-100 nm 3D silver nanostructures in a gelatin matrix," Nanotechnology **26**(12), 121001 (2015).
26. M. Terakawa, M. L. T. Mapa, A. Takami, D. Heinemann, N. N. Nedyalkov, Y. Nakajima, A. Hördt, T. Ripken, and A. Heisterkamp, "Femtosecond laser direct writing of metal microstructure in a stretchable poly(ethylene glycol) diacrylate (PEGDA) hydrogel," Opt. Lett. **41**(7), 1392–1395 (2016).
27. M. Machida, Y. Nakajima, M. L. T. Mapa, D. Heinemann, A. Heisterkamp, and M. Terakawa, "Shrinkable silver diffraction grating fabricated inside a hydrogel using 522-nm femtosecond laser," Sci. Rep. **8**(1), 187 (2018).
28. M. Machida, T. Niidome, H. Onoe, A. Heisterkamp, and M. Terakawa, "Spatially-targeted laser fabrication of multi-metal microstructures inside a hydrogel," Opt. Express **27**(10), 14657–14666 (2019).
29. K. Mizuguchi, Y. Nagano, H. Nishiyama, H. Onoe, and M. Terakawa, "Multiphoton photoreduction for dual-wavelength-light-driven shrinkage and actuation in hydrogel," Opt. Mater. Express **10**(8), 1931–1940 (2020).
30. W. Haiss, N. T. K. Thanh, J. Averard, and D. G. Fernig, "Determination of size and concentration of gold nanoparticles from UV-Vis spectra," Anal. Chem. **79**(11), 4215–4221 (2007).
31. L. Marcu, W. S. Grundfest, and J.-M. I. Maarek, "Photobleaching of arterial fluorescent compounds: characterization of elastin, collagen and cholesterol time-resolved spectra during prolonged ultraviolet irradiation," Photochem. Photobiol. **69**(6), 713–721 (1999).
32. H. N. Po and N. M. Senozan, "The Henderson-Hasselbalch equation: its history and limitations," J. Chem. Educ. **78**(11), 1499–1503 (2001).